International Journal of Thermofluids 22 (2024) 100641

Contents lists available at ScienceDirect

International Journal of Thermofluids

journal homepage: www.sciencedirect.com/journal/international-journal-of-thermofluids

Experimental investigation on diesel engine operating with CuO nanoparticles dispersed *Azadirachta indica* biodiesel

Ramu Garugubilli [a,c], Vanthala Varaha Siva Prasad [a], Jaikumar Sagari [b,*]

[a] *Department of Marine Engineering, Andhra University, Visakhapatnam, 530003, India*
[b] *Department of Mechanical Engineering, GITAM School of Technology, Visakhapatnam, 530045, India*
[c] *Department of Mechanical Engineering, Avanthi Institute of Engineering and Technology, Vizianagaram, India*

ARTICLE INFO

Keywords:
Cylinder pressure
Biodiesel
Cetane number
Nanoparticles
Carbon dioxide

ABSTRACT

This study aims to ascertain the operating parameters of a Copper oxide nanoparticle and *Azadirachta indica* biodiesel-powered diesel engine. Copper oxide nanoparticles were considered at 75 ppm, and three dispersants were added at the same ratio as nanoparticles. An ultrasonic bath sonicator was used to sonicate the nanoparticles, and later, the ultrasonicator was used to prepare the nanofuel. The experiment was conducted on a diesel engine with different injection timings, such as 21 °bTDC, 23 °bTDC, and 25 °bTDC at full load. The performance was slightly improved by mixing nanoparticles with B20, and it got even better by adding dispersants. The combustion parameters were also changed compared to diesel. Finally, the emissions of carbon monoxide, unburnt hydrocarbons, nitrogen oxides and smoke opacity were significantly reduced by the dispersion of nanoparticles. Increasing the injection timing also led to better results, and 25 °bTDC showed better results. The B20+CuO75+QPAN 75 has shown the most remarkable effects among other samples. At 25°bTDC, the brake thermal efficiency, brake specific fuel consumption, cylinder pressure, net heat release rate, were 35.03 %, 0.391 kg/kWh, 66.23 bar, and 89.39 J/°CA, respectively, while carbon monoxide, unburnt hydro carbons, smoke, and oxides of nitrogen were 0.089 %, 32 ppm, 19.351 %, and 1238 ppm.

1. Introduction

Diesel engines have many uses across several sectors, including industrial, agricultural, energy, and transportation. The superior productivity, reduced fuel consumption, and enhanced safety of the diesel engine account for this phenomenon. Furthermore, empirical research has shown that diesel engines are significant sources of harmful pollutants. These emissions have been shown to have harmful effects on the welfare of living species, so it is imperative that measures are taken to prevent their release. Today, global reserves of conventional fuels are running out and governments are increasingly prioritising the use of environmentally sustainable energy sources with potential for fuel production [1,2]. In recent years, global production and trade in biodiesel has increased significantly. Due to fluctuating crude oil prices and the uncertain supply of fuel over the past decade, coupled with the escalating cost of petroleum, there has been renewed interest in exploring vegetable oil alternatives for diesel engines. As biodiesel is an oxygenated fuel, unlike diesel, it can improve combustion characteristics and reduce pollutant emissions [3–5]. Basha et al. [6] investigated the production and combustion of biodiesel from a range of edible and non-edible vegetable oils. Despite its inedibility, Azadirachta indica oil has significant potential for production and availability, among other oil

Abbreviations: B100, Pure *Azadirachta indica* biodiesel; B20, 20% biodiesel and 80%diesel; NaOH, Sodium hydroxide; CuO, Copper oxide; CP, Cylinder pressure (bar); NHRR, Net heat release rate (J/°CA); BTE, Brake thermal efficiency (%); Ppm, Part per million; BSFC, Brake specific fuel consumption (kg/kWh); CR, Compression ratio; BP, Brake power (kW); CO, Carbon monoxide (%); UHC, Unburnt hydrocarbons (ppm); NO_x, Oxides of nitrogen (ppm); ASTM, American Society for Testing and Materials; SEM, Scanning electron microscope; mg/L, milli gram per litter; UV, Ultraviolet; nm, Nano metre; P, Instantaneous pressure of the cylinder (bar); C_p, Constant pressure specific heat (J/Kg K); Cv, Constant volume specific heat (J/Kg K); γ, Ratio of specific heat; HSU, Hartridge Smoke Unit; VCR, Variable compression ratio; CTAB, Cetyltrimethylammonium bromide; RSM, Response surface methodology; Cr_2O_3, Chromium oxide; ZnO, Zinc oxide; CeO_2, Cerium oxide; SiO_2, Silicon dioxide; Al_2O_3, Aluminium oxide; TiO_2, Titanium oxide; GO, Graphene oxide; NRL, Nano research lab; CuO75, 75 ppm CuO; QPAN75, 75 ppm QPAN80; TWEEN75, 75 ppm TWEEN; TRITONX75, 75 ppm TRITONX.

* Corresponding author.
E-mail address: sagari.jaikumar1@gmail.com (J. Sagari).

https://doi.org/10.1016/j.ijft.2024.100641

Available online 25 March 2024

options. The transesterification-based biodiesel synthesis from Azadirachta indica and Pongamia oils was optimised by Vinayaka et al. [7] using Response Surface Methodology (RSM). Using a fuel blend containing gaseous fuels, alcohols, and nanoparticles can potentially improve performance and reduce emissions. Several tests have shown that the use of nanoparticles in biodiesel leads to improved combustion and lower emissions [8,9]. Nanoparticles that are stable in liquids are necessary for their application as a thermophysical and heat transfer medium in liquid fuels. Various complex approaches are described in the scientific literature to increase nanoparticle stability while suspended in the base liquid. Some of these methods include surface modification and ultrasonic treatment [10,11]. Nema et al. [12] included cetyltrimethylammonium bromide (CTAB) in the process of producing nanofuel using Al_2O_3 nanoparticles as an additive. They discovered that the dispersion stability of the particles prepared from Al_2O_3 was sufficient. Jagadish et al. [13] investigated the stability of chromium oxide (Cr_2O_3) nanoparticles in *Mesua ferrea* biodiesel. They found that when QPAN 80 was combined with CTAB, both the dispersant and the nanofuel were more stable. The addition of Cr_2O_3 nanoparticles to the fuel also improved its properties. Madhavi et al. [14] used Titanium oxide (TiO_2) nanoparticles to study the effects of using *Semecarpus anacardium* biodiesel. They found that the dispersant is crucial for achieving the desired level of stability and that it is impossible without it. Praveena et al. [15] investigated how the properties of grape seed biodiesel change when Zinc oxide (ZnO) and Cerium oxide (CeO_2) nanoparticles are added to the fuel. They found that the calorific value was significantly altered, and other measured variables were also dramatically affected. This discovery was in addition to the fact that there was an effect on the calorific value.

Jaikumar et al. [16] investigated the effects of Cr_2O_3 nanoparticles in linseed biodiesel in a diesel engine. They found a significant improvement in combustion characteristics. Engine performance was improved while environmental pollution was reduced. Nanthagopal et al. [17] investigated ZnO and TiO_2 nanoparticles and biodiesel. It was shown that the brake thermal efficiency could be enhanced while engine emissions were significantly decreased. In addition, the addition of nanoparticles increased the cylinder pressure. Perumal et al. [18] investigated the effects of adding nanoparticles of metal oxides such as Silicon dioxide (SiO_2), Aluminium oxide (Al_2O_3), and Titanium oxide (TiO_2) to a mixture of used cooking oil and biodiesel. They noted that the positive results for combustion and performance were established together with emissions. The researchers discovered significant improvements in nanoparticle dispersion and combustion characteristics. In addition, pollutant emissions have been reduced, and engine performance has improved. Praveen et al. [19] studied pongamia biodiesel and Copper oxide (CuO) nanoparticles. It was found that the performance was enhanced, and emissions were reduced. Illipilla et al. [20] studied *Semecarpus anacardium* biodiesel dispersed with TiO_2 nanoparticles. They concluded that performance increased markedly and exhaust emissions decreased significantly. Jaikumar et al. [21] studied the effects of Al_2O_3 nanoparticles with dispersants in biodiesel. They found that the increased stability was the main reason for the observed more significant improvement in combustion characteristics. Pala et al. [22], who also looked at the physicochemical properties, examined the stability of graphene oxide (GO) nanoparticles in mahua biodiesel blends. They showed that stability was increased by adding dispersant to the GO nanoparticles. Reddy et al. [23] investigated biodiesel in diesel engine using SiO_2 nanoparticles and *Abrus precatorius*. They reported that performance and combustion parameters were improved while emissions were reduced. Moreover, the output parameters predicted by Response Surface Methodology (RSM) agree well with the experimental results.

Several studies have been carried out on the effects of various nanoparticles in biodiesel, building on earlier findings. Nevertheless, the stability properties of nanoparticles introduced into liquid fuels need to be further investigated. Several studies have been conducted with different oxide nanoparticles, but very few studies [18,22,23] have dealt with the surface modifications by surfactants and dispersants in terms of stability. Moreover, the CuO nanoparticles have higher thermal conductivity, which could improve the combustion properties, and higher catalytic activity than the other oxide nanoparticles, which enhances the combustion properties. So, this study looked at adding different surfactants, like TRITONX, QPAN80, and TWEEN80, to Azadirachta indica biodiesel blend (B20) to stabilize the CuO nanoparticles. In addition, the operation of diesel engine with CuO nanoparticles dispersed in *Azadirachta indica* biodiesel was evaluated by changing the injection timing. The influence of injection timing is also a new combination with nanofuel in diesel engine applications.

2. Materials and methods

This section deals with the materials used, the production of biodiesel from crude *Azadirachta indica* oil, the characterisation of nanoparticles, the production of nanofuel, stability tests, tests of physicochemical properties and experiments with direct injection diesel engines.

2.1. Materials

The oil from the seeds of *Azadirachta indica* (Fig. 1) was used in this study and was obtained from Sivaroma Naturals Pvt. Ltd., India. Other materials and chemicals like NaOH catalyst, methanol as alcohol, hexane as solvent, CuO nanoparticles, TRITONX, QPAN80 and TWEEN 80 as dispersant were used in the present study. The CuO nanoparticles were obtained from Nano Research Lab (NRL), Jharkhand, India.

2.2. Transesterification process

The purified seed oil of *Azadirachta indica* was used to produce biodiesel through a chemical transesterification process. The crude neem oil was subjected to a thermal process in which the temperature was raised to 50°C. It was then subjected to chemical treatment with a catalyst of sodium hydroxide (NaOH) and a mixture of methanol. To achieve homogeneity, the entire solution was stirred with a magnetic stirrer. The reaction was carried out over 60 min under isothermal conditions at a fixed temperature of 65^{o}C. After completion of the reaction, the glycerol was separated from the methyl ester using a separating funnel. The moisture content of the biodiesel was removed by washing with hot water at a temperature of 90°C. Fig. 2 shows a schematic representation of the biodiesel production process.

2.3. Characterization of CuO nanoparticles

2.3.1. SEM

The nanoparticles were characterised using a scanning electron microscope (SEM). Fig. 3 shows the SEM images of the CuO nanoparticles. The image shows the surface morphology of the material, which results from the complicated interaction of atoms and electrons inside the substance. The determination of the crystalline structure of the CuO nanoparticle can be deduced from the areas of lower intensity in the image.

2.3.2. XRD

The XRD pattern of the copper oxide nanoparticles is shown in Fig. 4. The pattern shows a sharp and rigid peak ($2\theta = 35.628°$) corresponding to the typical cubic crystal structure, with the dominant peaks at (110), (111) and (220), as shown in the figure. The observed strong peak is in good agreement with the estimated intercellular distance derived from the XRD results for these nanoparticles: $d = 2.5180$ Å for the (1 1 1) plane.

The Scherrer equation was applied to the XRD data to determine the mean size of the CuO nanoparticles. The particle size is calculated using the following Eq. (1):

Fig. 1. *Azadirachta indica* plant and seeds.

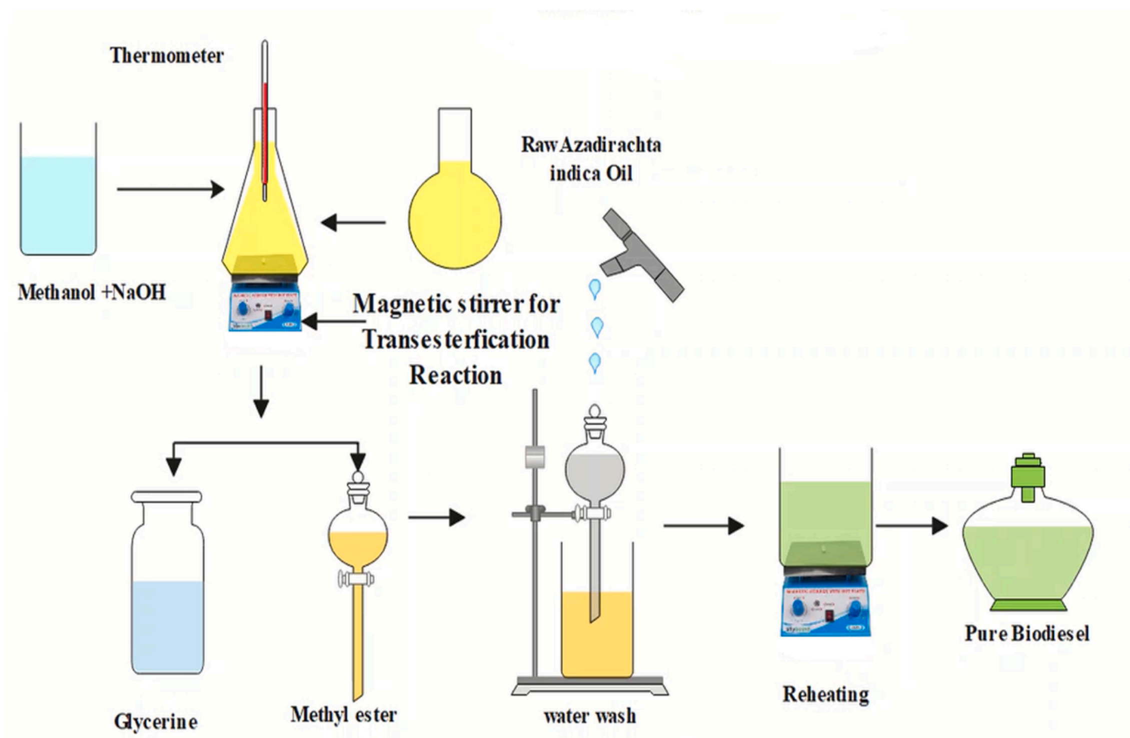

Fig. 2. Transesterification procedure.

$$D = K\ \lambda/\beta\ cos\theta \quad (1)$$

Where K stands for the shape factor, λ for the wavelength of the X-ray beam, the Bragg diffraction angle and the FWHM value. The determination of the crystallite size of CuO nanoparticles resulted in a value of 20.86±0.08 nm.

2.4. CuO nanofuel preparation

First, a solution containing 75 ppm CuO nanoparticles was placed in a small container and subjected to ultrasonic treatment with the solvent hexane. Additional CuO nanoparticles were added to the system with various dispersants, including TRITONX, QPAN80 and TWEEN 80. The sample was subjected to a drying process at a temperature of 35, for 30 min. Also, 20 % Azadirachta indica biodiesel (B20) and copper oxide (CuO) nanoparticles were mixed to make the nanofuel samples. The procedure was carried out using an ultrasonic probe sonicator at a frequency of 45 Hz.

2.5. Stability test

The stability of the test fuel samples was evaluated with a UV spectrophotometer using the spectral transmission method in a wavelength range of 200–1100 nm over a period of three consecutive weeks. Fig. 5 (a)-(c) illustrates the relationship between absorbance with respect to wavelength. Instability of the CuO nanoparticles was observed over the period from week 1 to week 3, independent of the fuel samples.

The light transmittance of B20+CuO75, B20+CuO75+TRITONX 75, B20+CuO75+QPAN75, and B20+CuO75+TWEEN75 was 93.75 %, 89.29 %, 86.03 %, and 91.56 % at week 1, 95.75 %, 90.29 %, 88.03 %, and 93.56 % at week 2, and 98.75 %, 94.29 %, 92.06 %, and 96.56 % at week 3, respectively.

2.6. Properties of fuel samples

The nanofuel samples' properties were evaluated according to the

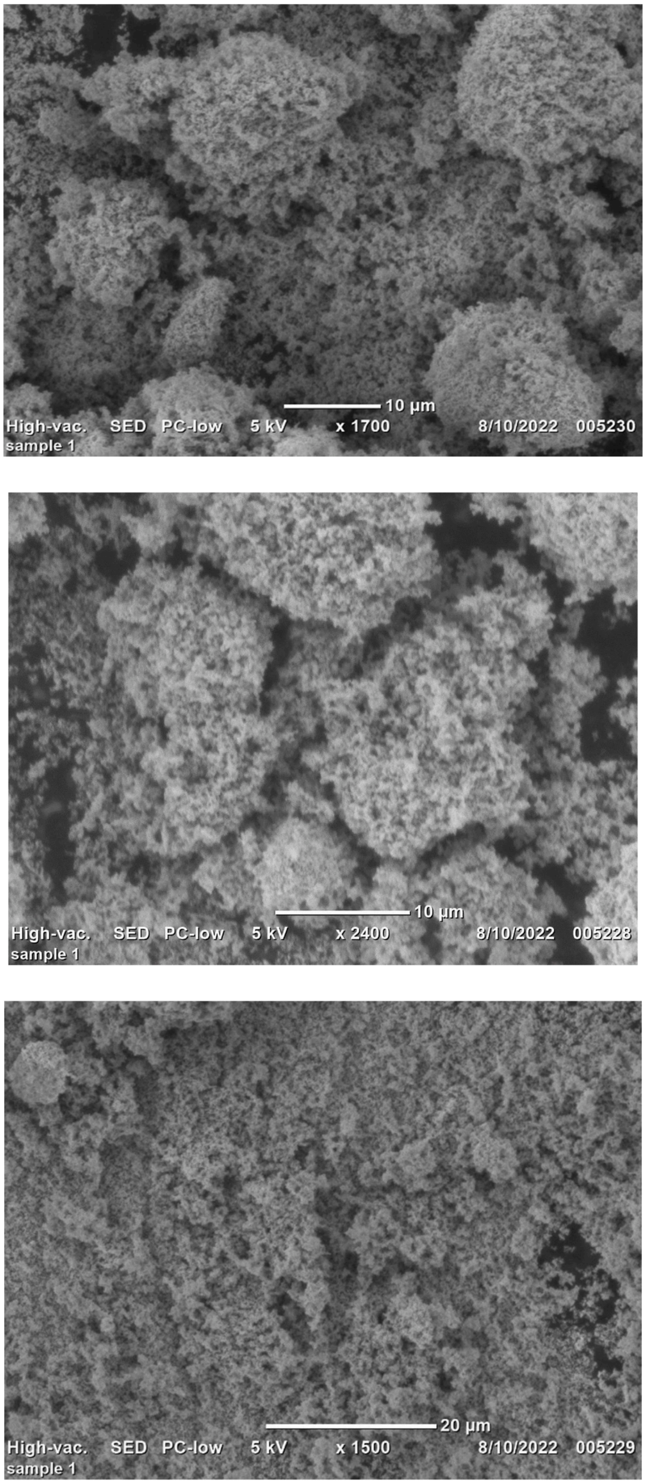

Fig. 3. SEM images of CuO nanoparticles.

criteria established by the American Society for Testing and Materials (ASTM). The results of this evaluation are shown in Table 1. Nanoparticles have been suggested as a potential approach to improve the calorific value and cetane number of fuels. Conversely, density, kinematic viscosity, and flash point have been shown to have a minor unfavorable character. Incorporating CuO nanoparticles in conjunction with using various dispersants resulted in a significant increase in both the calorific value and cetane number of B20. In addition, dispersants such as TRITONX, QPAN 80 and TWEEN 80 in CuO nanoparticles were found to improve the properties of B20, particularly in terms of cetane

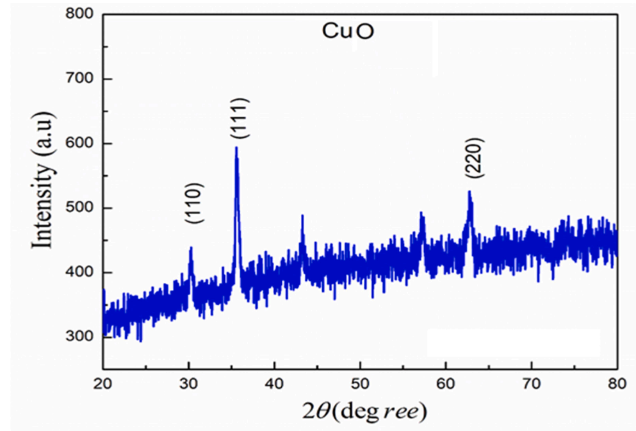

Fig. 4. XRD of CuO nanoparticles.

number and heating value. The observed phenomenon can be attributed to the improved stability of B20 and the homogeneous dispersion of the nanoparticles in the material. In addition, it is worth noting that the dispersants had HLB values in the range of 8–15, suggesting a homogeneous distribution of the oil in the solution. The maintenance of stability and improvement of physicochemical properties of CuO nanoparticles can be reasonably inferred from their dispersion. The fuel containing nanoparticles significantly increases calorific value and cetane number. The fuel blend of B20, CuO75 and QPAN 75 exhibited higher cetane number and heating value of 60 and 40,012 kJ/kg K, respectively.

2.7. Experimental setup

Fig. 6 is a schematic representation of the experimental setup. A single-cylinder four-stroke engine with direct injection and compression ignition is used in this study. Table 2 contains the technical data for the engine. Diesel and the nanoparticle-based fuel were stored in special tanks. A load bank fed dynamometer had the engine connected to it. Exhaust emissions were measured with a gas analyser (model MARS 5) and a smoke metre. A personal computer (PC) was connected to all measurement sensors via an analogue-to-digital converter (ADC). Ten PC cycles were used to analyse the combustion parameters with the integrated Enginesoft software. The net heat release can be calculated with Eq. (2) according to the first law of thermodynamics.

$$\frac{\Delta Q}{\Delta \theta} = \frac{\Delta P}{\Delta \theta}\,\frac{1}{\gamma - 1} + P\frac{\Delta V}{\Delta \theta}\,\frac{\gamma}{\gamma - 1} + \frac{\Delta Q\ HEAT}{\Delta \theta} \tag{2}$$

Where, $\gamma = \frac{CP}{CV}$, $\frac{\Delta P}{\Delta \theta}$ is pressure variation compared to crank angle (m^3/degree), $\frac{\Delta V}{\Delta \theta}$ volume variation versus crank angle (m^3/degree), $\frac{\Delta Q\ HEAT}{\Delta \theta}$ is the rate of heat transfer along the walls of the combustion chamber (J/°CA), V and Pare the cylinder's instantaneous volumes (m^3) and pressures (bar), C_V and $C_{P.}$

Before commencing the test, the engine was operated using diesel fuel for 15 min to achieve a stable condition. The entire test was performed at full load (100 %) and a speed of 1500 rpm. The standard diesel was tested first, then the BD20, and finally, the nano fuels. The entire study was conducted with three different injection times (ITs) of 21 °bTDC, 23 °bTDC, and 25 °bTDC. The engine was run for 10 min before each measurement, and the experiments were repeated multiple times and presented the average values for accuracy.

3. Results and discussions

The present section deals with the discussion of the experimental results regarding the performance, combustion and emission characteristics of a direct injection diesel engine operated with different

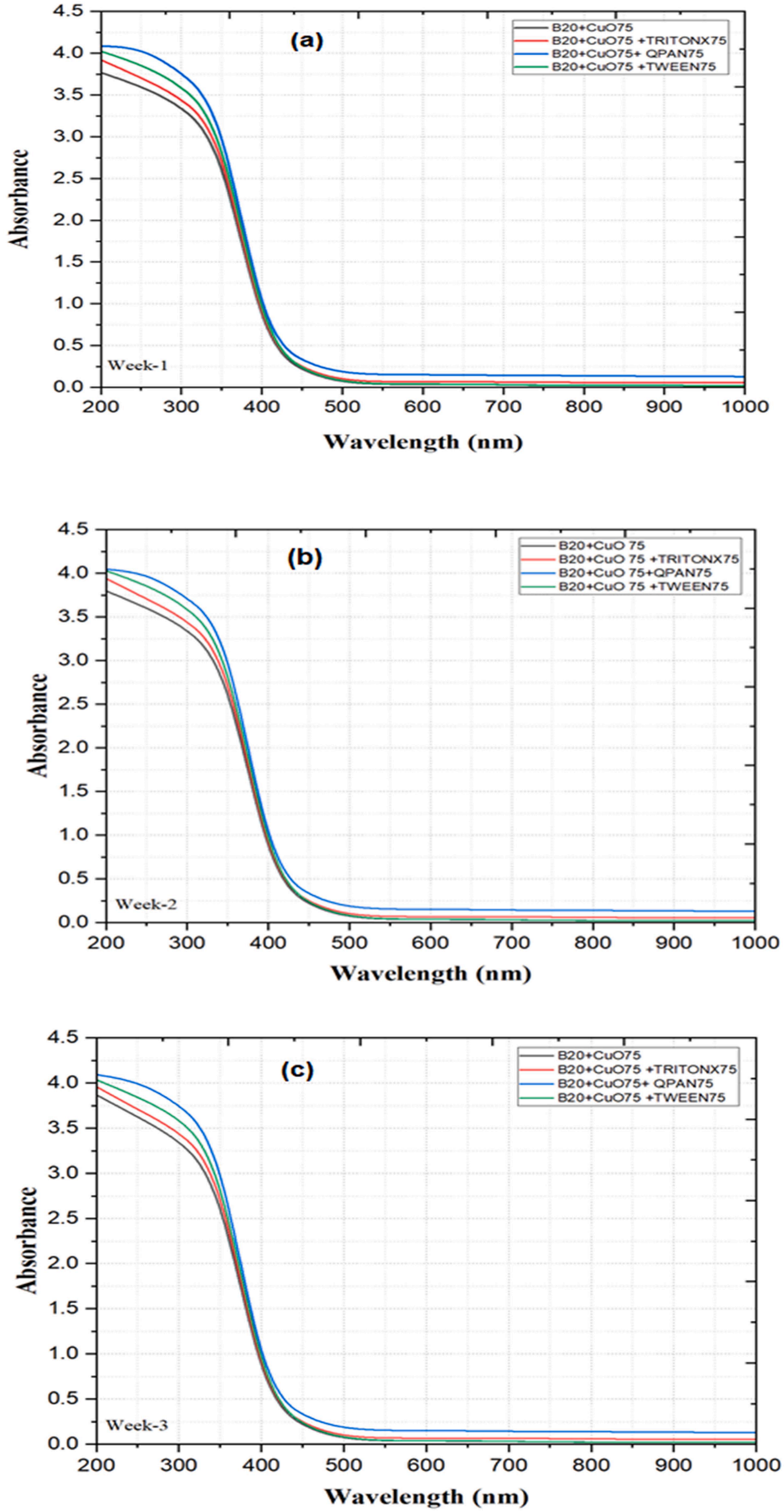

Fig. 5. Transmittance at (a) week 1 (b) week 2 (c) week 3.

Table 1
Fuel properties.

Fuel property	Relative density at 15 °C (kg/m³)	Calorific value (kJ/kg)	Viscosity at 40°C (Cst)	Cetane number	Flash point (°C)	Copper corrosion
Testing method	ASTMD-1298	ASTMD-4809	ASTMD-445	ASTMD-976	ASTMD-92	ASTMD-130
ASTM range	860–910	42,000	2.4–7	48 (min)	135 (min)	1a
B20	862	38,719	3.68	57	146	1a
B20+CuO75	869	39,928	3.95	58	144	1a
B20+CuO75+TRITONX	871	39,944	3.962	59	142	1a
B20+CuO75+QPAN 75	868	40,012	3.944	60	143	1a
B20+CuO75+TWEEN 75	872	39,942	3.96	59	141	1a

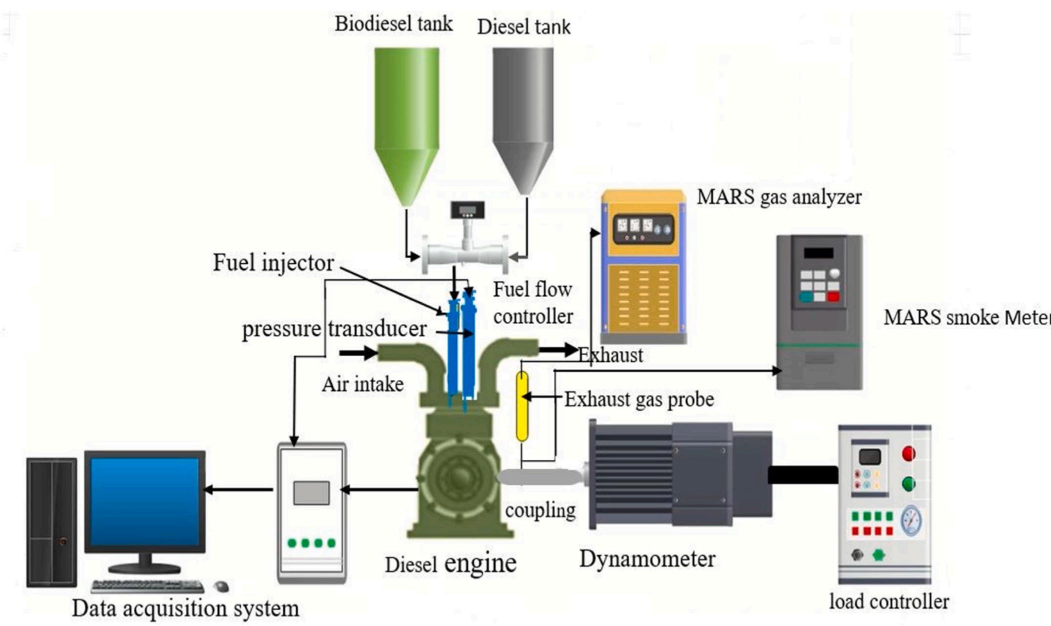

Fig. 6. Pictorial view of test rig.

Table 2
Specifications of the engine.

Parameter	Description
Type of engine	TAF-1, Kirloskar, VCR diesel engine
Brake power (kW)	3.5
Cylinders	1
Engine load	100 % load
Bore (mm)	87.5/110
Stroke (mm)	110
Compression ratio and Injection pressure (bar)	17.5 and 200 bar
Injection timings	21 °bTDC, 23 °bTDC, and 25 °bTDC
Speed (rpm)	1500

injection timings. BTE and BSFC are the performance parameters, CP and NHRR are the combustion characteristics and CO, UHC, NO_x and smoke are the emission characteristics.

3.1. Performance parameters

3.1.1. BTE

Fig. 6 shows the variation in BTE against injection timing. The BTE of B20 was similar to that of conventional diesel due to the undesirable atomization of the fuel and lower heating value [22,23]. However, the BTE increased sharply when CuO nanoparticles were introduced into B20. The dispersion of CuO nanoparticles increased the calorific value of the fuel mixture. Also, the enhancement of thermal conductivity of CuO nanoparticles leads to improved combustion characteristics and increased heat transfer, both of which improve BTE [26,27]. Therefore, using B20 fuel containing dispersed CuO nanoparticles instead of conventional diesel fuel can effectively improve the production and conversion of chemical energy. As a result, the BTE has been significantly improved. The increased surface-to-volume ratio is one of the factors contributing to higher BTE [28–30]. Due to their greater stability with added surfactants and dispersants, nanoparticles have further improved BTE. This is associated with the improved ignition properties of B20 [31,32]. The increase in BTE can be attributed to the improved combustion resulting from the injection timing increase, which led to better atomization and vaporization. The highest BTE, regardless of the test fuels, was noted at an IT of 25 °bTDC. Diesel, B20, B20+ CuO75, B20+CuO75+ QPAN75, B20+CuO75+TRITONX75, B20+CuO75+ TWEEN75 had BTEs of 29.97 %,30.89 %,31.92 %,33.81 %,32.76 %, and 35.03 %, respectively, at an IT of 25 °bTDC. BTE of the tested fuel B20+ CuO+75+QPAN75 was higher than that of the other test samples.

3.1.2. BSFC

Fig. 7 shows the BSFC regarding injection timings. Because of its greater viscosity and lower calorific value, B20 has been found to possess more BSFC over regular diesel fuel [33]. Unlike conventional diesel fuel, the dispersion of CuO nanoparticles in B20 decreased BSFC due to enhanced fuel properties, especially calorific value. When CuO nanoparticles were mixed with B20 diesel fuel, the BSFC went down because the fuel's properties got better, especially its calorific value [34]. Because the fuel mixture contained more oxygen, combustion was much more complete when CuO nanoparticles were used, contributing to the lower BSFC. Nanoparticles could also lead to a decrease in

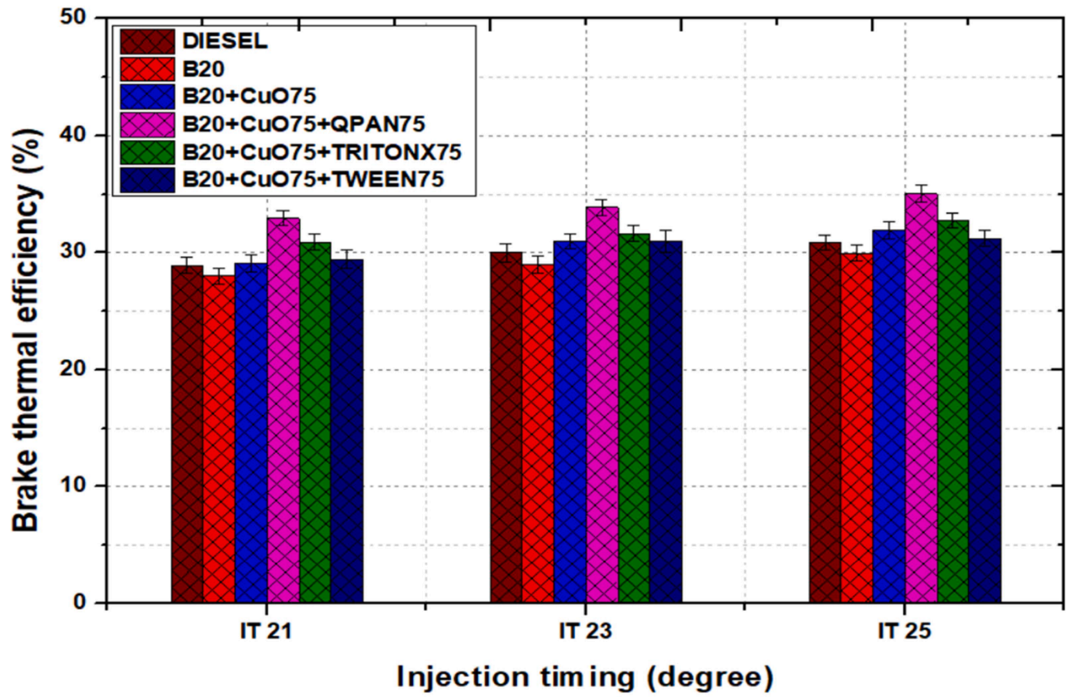

Fig. 7. BTE against injection timing.

brake-specific fuel consumption (BSFC). Nanoparticles provide many benefits compared to the basic fuel, including an increased surface-to-volume ratio, enhanced thermal conductivity, and improved utilization of the chemical energy present in the fuel [1,9]. Furthermore, the addition of dispersants and surfactants led to a significant decrease in BSFC due to the exceptional stability of CuO nanoparticles in liquid fuel [9,10,25]. BSFC decreased with the increase of injection timing from 21 °bTDC to 25 °bTDC due to better fuel atomization, resulting in more efficient combustion.

The BSFC of diesel, B20, B20+CuO75, B20+CuO75+ QPAN75, B20+CuO75+TRITONX75, B20+CuO75+TWEEN75 were 0.417 kg/kWh,0.421 kg/kWh, 0.415 kg/kWh, 0.395 kg/kWh, 0.401 kg/kWh, and 0.391 kg/kWh at an injection timing of 25 °bTDC, respectively. The samples with the lowest BSFC were B20+ CuO75+QPAN75.

3.2. Combustion parameters

3.2.1. Cylinder pressure (CP)

Fig. 8(a) and (b) illustrate the variation of the CP as a function of crank angle and injection timing. B20 has a slightly higher CP than

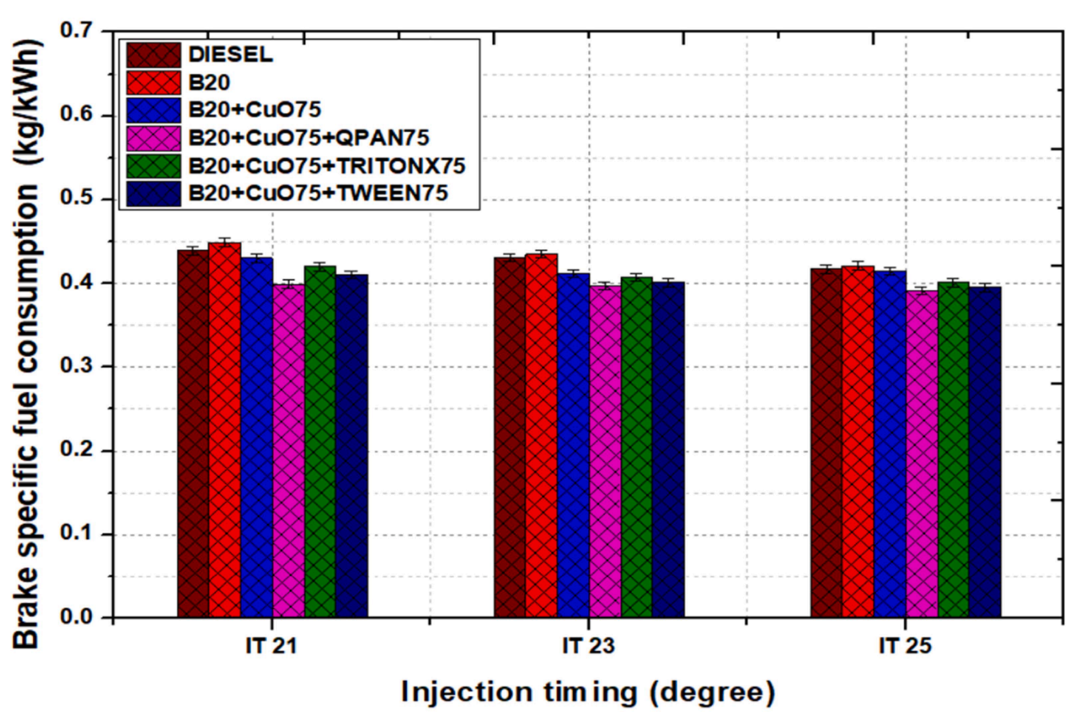

Fig. 8. BSFC against injection timing.

standard diesel, which is due to the fact that it has a higher cetane number and is more oxygenated than normal diesel [10].

However, due to the higher thermal conductivity and the larger surface-to-volume ratio of the nanoparticles, their dispersion in B20 led to an even greater increase in CP. [25,27]. Due to better fuel mixing and uniformity, the oxygenated imprint of CuO nanoparticles in B20 may also significantly impact the growth of CP [3,16,26].

The increased stability of the CuO nanoparticles in the B20 mixture led to a significant improvement in CP when a dispersant and surfactant were used, possibly also improving combustion and mass transfer properties [3,9.16]. Improved oxidation and combustion was achieved by increasing the injection timing, allowing more fuel to accumulate and more time for better mixing. This allowed the cylinder pressure to be increased

The cylinder pressure of diesel, B20, B20+CuO75, B20+CuO75+QPAN75, B20+CuO75+TRITONX75, B20+CuO75+TWEEN75 were 58.38 bar, 60.84 bar, 64.43 bar, 62.83 bar, and 66.23 bar respectively at an injection timing of 25 °bTDC. Comparing the test samples, BD20+ CuO75+QPAN75 was able to reach the highest cylinder pressure.

3.2.2. Net heat release rate (NHRR)

Fig. 9(a) and (b) show the change in NHRR as a function of crank angle and injection time, respectively. The NHRR for B20 is slightly better than that of conventional diesel. B20 has a slightly higher NHRR than diesel because it has a higher cetane number and contains more oxygen than diesel [3,20,21]. More fuel is formed due to the ignition delay, which increases the heat release rate [20]. There was significantly improvement in NHRR when the CuO nanoparticles were added to B20. This was due to the catalytic properties of the fuel and the enhanced heat transfer from the CuO nanoparticles to B20 [3,16]. In addition, the higher NHRR is due to the nanoparticles' higher surface/volume fraction [8,29]. The mixture of dispersant and surfactant also significantly improved the NHRR because of the increased stability of nanoparticles

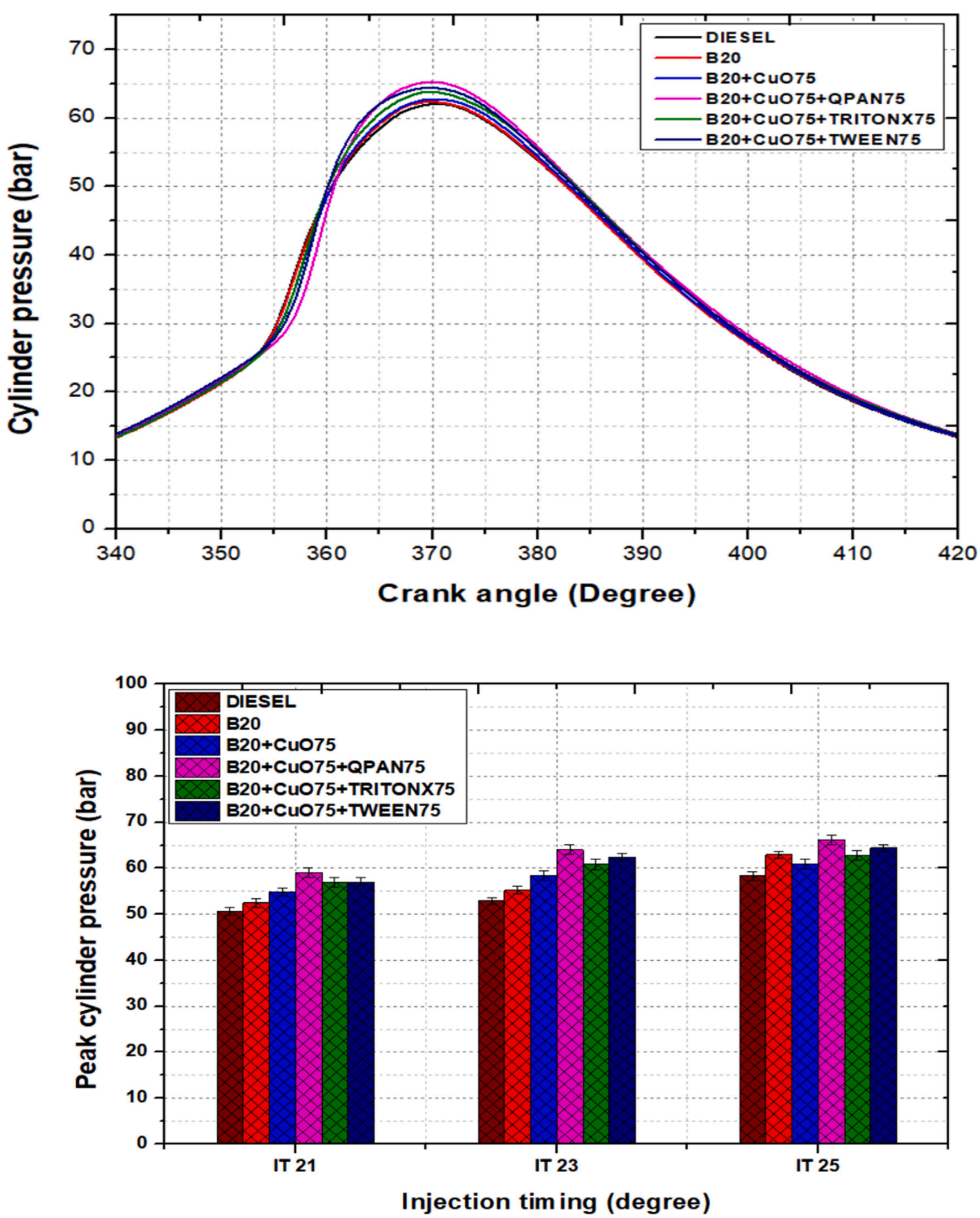

Fig. 9. CP versus (a) crank angle (b) injection timing.

in BD20 [25]. The NHRR increased with the increase in injection timing. This was due to increased fuel accumulation during advanced injection and subsequently increased fuel consumption during the premixing combustion phase, resulting in a higher heat release rate. This pattern was the same for all samples of blended test fuel. The result is a higher heat release rate due to temperature and pressure taking precedence in the cylinder.

At an injection timing of 25 °bTDC, the NHRR of diesel, B20, B20+ CuO75, B20+CuO75+ QPAN75, B20+CuO75+TRITONX75, and B20+CuO75+TWEEN75 were 74.88 J°/CA, 77.76 J/°CA, 80.56 J/°CA, 83.91 J/°CA,86.24 J/°CA, and 89.39 J/°CA, respectively. The highest NHRR was found in B20+ CuO75+QPAN75.

3.3. Emission characteristics

3.3.1. Carbon monoxide (CO)

Fig. 10 displays the change in CO values for various test gasoline blends as a function of injection timing. The primary constraint on CO emissions is the stoichiometric air-fuel ratio. In addition, inefficient temperature and fuel-air mixture lead to an increase in CO generation

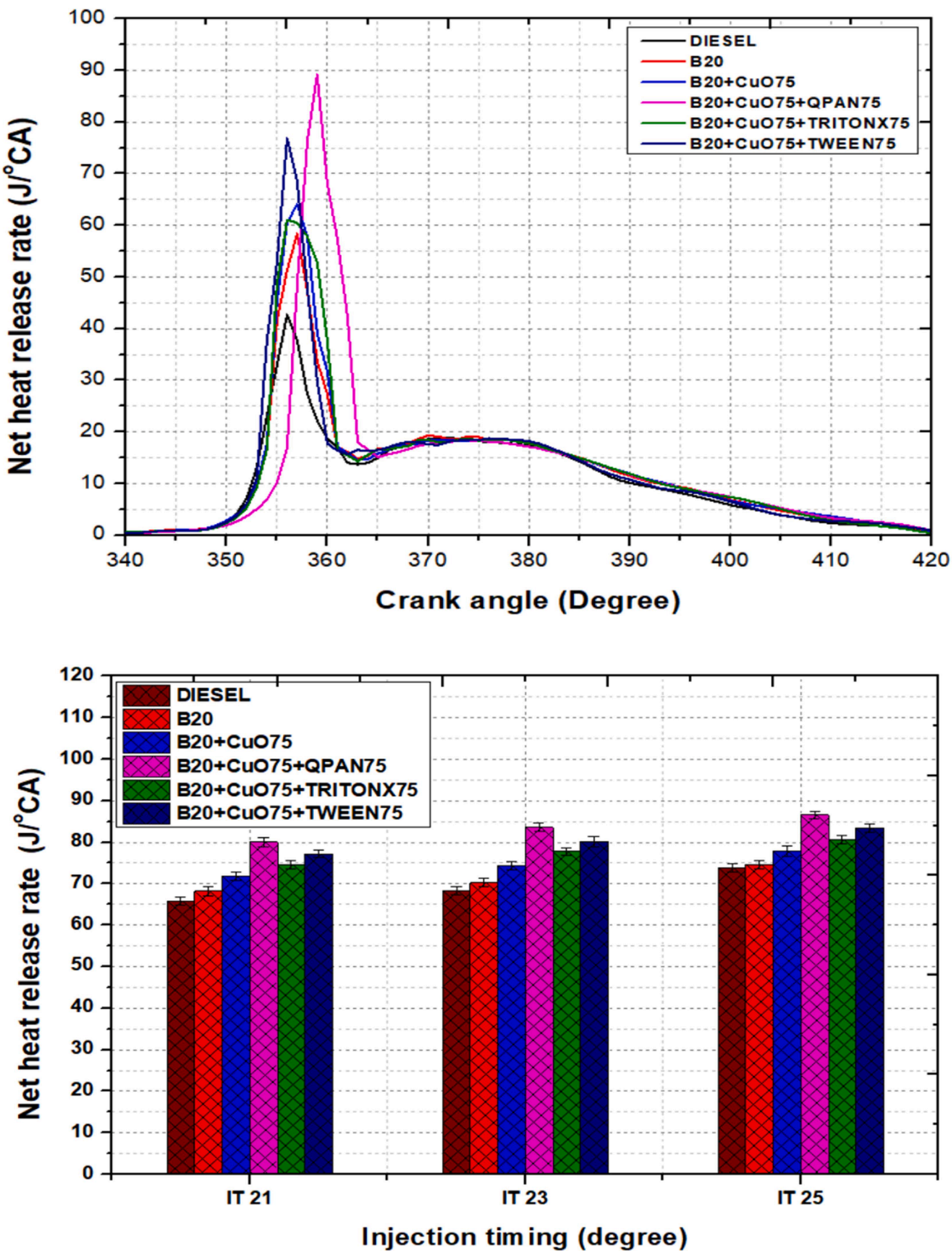

Fig. 10. NHRR versus (a) crank angle (b) injection timing.

[8]. The CO content of B20 was lower than that of conventional diesel fuel. This was attributed to the higher cetane number and the oxygenated fuel blend due to the higher oxygen availability [10,20,33]. The dispersion of CuO nanoparticles in B20 further lowered the CO values. The improvement of ignition properties, catalytic movement, surface area, improved chemical reactivity and reactive oxygenation [8,9,16,24].

CO production was further reduced in the case of dispersant-added non-fuel, as the CuO nanoparticles could persist in B20 [10,16,24,25]. Extending injection timing increases the cylinder temperatures and accelerates the oxidation of carbon and oxygen, which leads to lower CO emissions even at high combustion rates. As a result, CO emissions are reduced. At an injection timing of 25°bTDC Diesel, B20, B20+ CuO75, B20+CuO75+ QPAN75, B20+CuO75+TRITONX 75, B20+CuO75+TWEEN75 had CO of 0.138 %,0.129 %,0.119 %,0.101 %,0.113 % and 0.089 % percent, respectively. The test sample BD20+ CuO75+QPAN75 had the least CO in compared to the other test samples.

3.3.2. Unburnt hydrocarbons (UHC)

The UHC for fuels containing distributed CuO nanoparticles with respect to injection timing is shown in Fig. 11. Oxygen deficiency and high combustion temperatures contribute to higher UHC emissions. Since incomplete fuel combustion produces more UHC [8] incomplete fuel combustion is harmful.

UHC greatly reduced the ability of CuO nanoparticles to disperse in B20 [25]. UHC significantly reduced the ability of CuO nanoparticles to disperse in B20. The air-fuel mixture was more prominent, and the fuel burned more efficiently due to adding nanoparticles. Furthermore, the oxygen content of the CuO nanoparticles can improve combustion [25,31]. The increased surface area of the oxide group nanoparticles generated may promote complete fuel combustion [8,25], which was another factor for the reduced UHC. Due to better dispersion of the nanoparticles, the UHC of the surface-modified CuO nanoparticles in B20 was significantly reduced [25]. UHC also decreased substantially as a result of increasing the injection timing. This was cited as a cause of better fuel atomization. The same symptoms were also attributed to the full test patterns. The UHC of diesel, B20, B20+CuO75, B20+CuO75+QPAN75, B20+CuO75+TRITONX75, B20+CuO75+TWEEN75 were 42 ppm, 40 ppm, 38 ppm, 34 ppm,36 ppm, and 32 ppm. The UHC was lower in BD20+ CuO75+ QPAN75 than in the residual samples.

3.3.3. Oxides of nitrogen (NO_x)

Fig. 12 shows the variation of NO_x values as a function of injection timing. The NO_x level of B20 is a little higher compared to regular diesel.

B20 has more oxygen, higher combustion temperature, and higher cetane number [8]. However, a significant reduction in NO_x levels was observed when CuO nanoparticles were mixed with B20. This phenomenon is due to improved heat transfer and the ability of nanoparticles to store thermal energy, resulting in a lower average temperature of the cylinder compared to conventional diesel fuel [25]. The NO_x values increased at higher injection timing due to the higher combustion temperatures. All test samples used in the analysis showed the same pattern, and higher injection timing followed the progressive reduction. NO_x at an injection timing of 25 °bTDC was 1502 ppm, 1467 ppm, 1387 ppm, 1286 ppm,1304 ppm and 1238 ppm for Diesel, B20, B20+CuO75, B20+CuO75+ QPAN75, B20+CuO75+TRITONX75, B20+CuO75+TWEEN75, respectively. The combination of test fuels with the lowest NO_x emissions was B20+CuO75+QPAN75.

3.3.4. Smoke

Fig. 13 shows the variation of the injection timing for the smoke. The smoke opacity was significantly lower with B20 than with diesel.

The main reason for the reduction in smoke generation was the oxidised nature of B20 [16,20,32]. Since B20 contains CuO nanoparticles, the amount of smoke generated by excessive oxygen was reduced. Also, the dispersant-added CuO nanoparticles in B20 had lower smoke production due to improved dispersion of the nanoparticles [25]. The larger injection timing also helped to lower the expected smoke for all test samples by improving combustion. At an injection timing of 25 °bTDC, the smoke of diesel, B20, B20+CuO75, B20+CuO75+ QPAN75, B20+CuO75+TRITONX75, B20+CuO75+TWEEN75 produced smoke

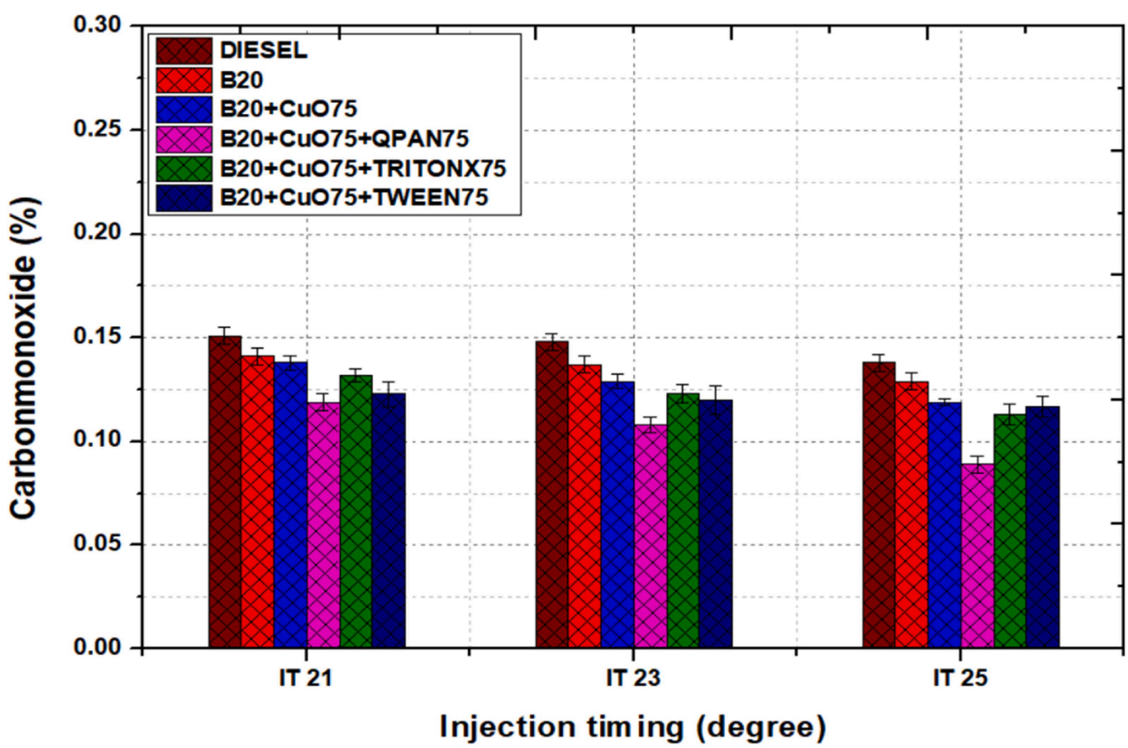

Fig. 11. CO at different injection timings.

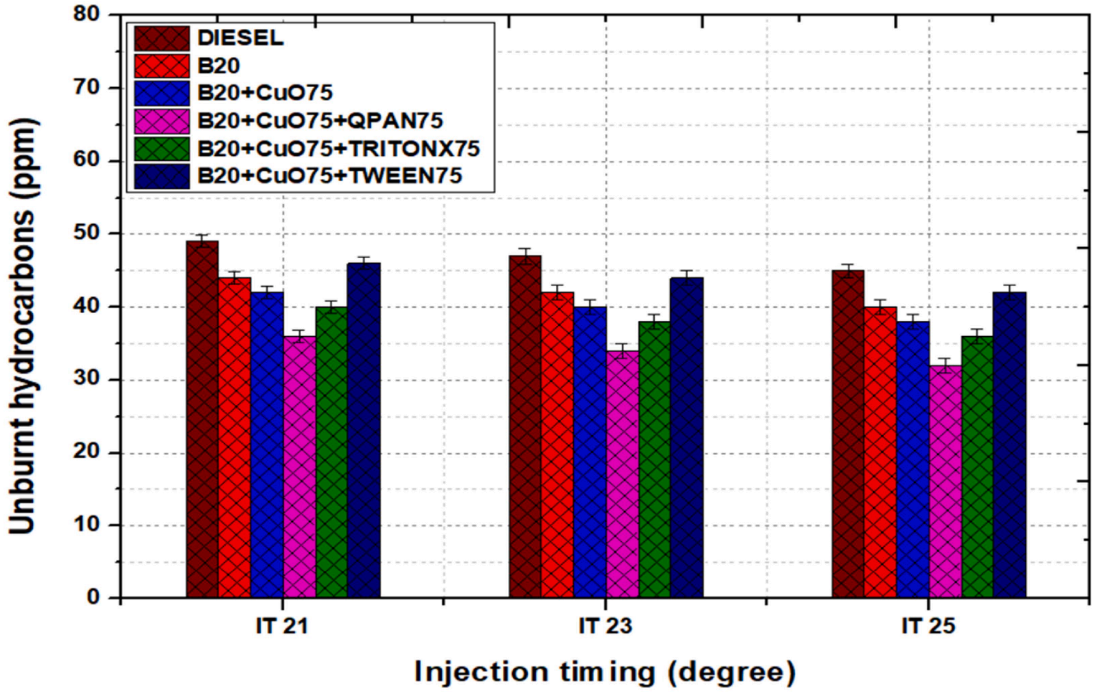

Fig. 12. UHC at different injection timings.

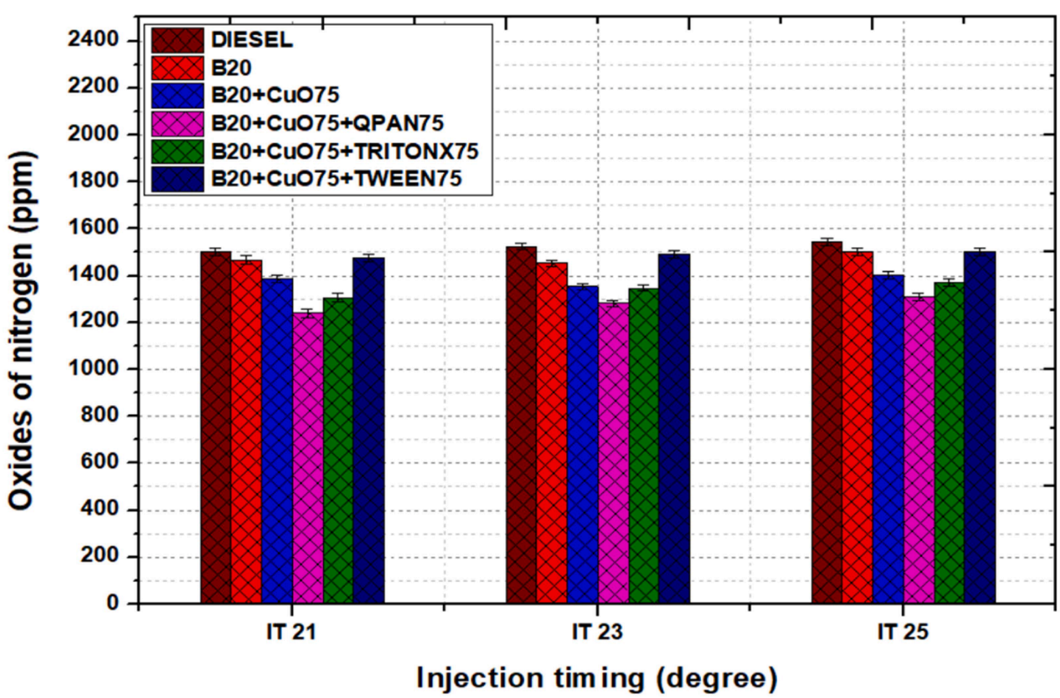

Fig. 13. NO_x at different injection timings.

with respective smoke percentages of 36.312 %, 32.245 %, 29.239 %, 22.124 %,26.396 % and 19.351 %. Among all the test fuels, BD20+ CuO75+ QPAN75 created the least smoke. Fig. 14

4. Conclusions

The aim of this study was to evaluate the combustion, performance, and emission characteristics of diesel engines using biodiesel samples with entrapped CuO nanoparticles. Upon completion of the study, the following findings were obtained:

- *Azadirachta indica* biodiesel (B100) and its blend (B20) were found to have better cetane number than conventional diesel.
- The dispersion of CuO nanoparticles in B20 using the dispersants improved the stability of the nanoparticles so that the nanoparticles were more stable overall. It was found that the dispersion had a better effect on the stability of the CuO nanoparticles than the base nanoparticles themselves. Dispersant and CuO nanoparticles were used as part of the formulation process to achieve the desired results of decreased permeability and increased absorption. On the other hand, the dispersant QPAN 80 added to biodiesel blend showed

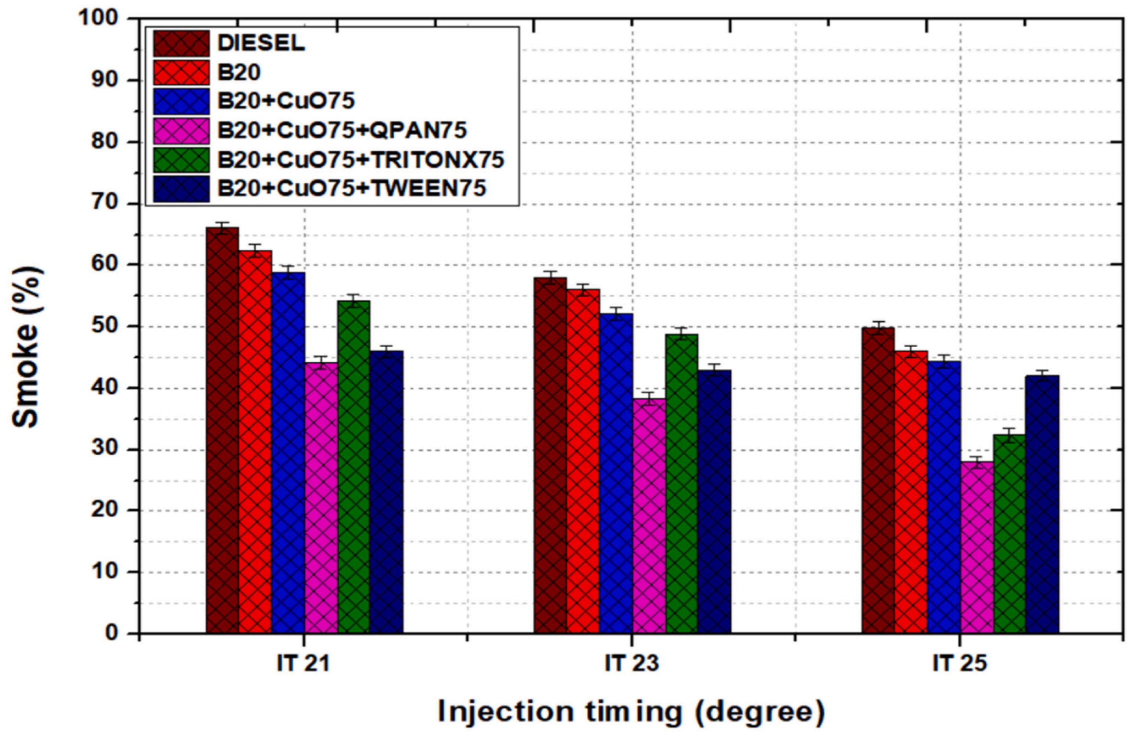

Fig. 14. Smoke at different injection timings.

greater particle stability than the additional particles of TRITONX and TWEEN 80 in B20. The permeability of the combination B20+CuO75+QPAN75 was lower at 86.03 %, while the absorption was higher at 4.08 %.

- Both the calorific value and the cetane number were estimated to be higher than they were 40,012 kJ/kg and 60, respectively.
- The BTE increased while the BSFC decreased when CuO nanoparticles were mixed with B20. At an injection time of 25 °bTDC, B20+CuO75+QPAN75 exhibited developed BTE and minimum BSFC of 35.03 % and 0.391 kg/kWh, respectively.
- The dispersion of nanoparticles in B20 significantly increased CP and NHRR of combustion. The best results were obtained with the combination of B20+ CuO75+QPAN75. The extreme CP and NHRR of B20+CuO75+QPAN75 were 66.23 bar and 89.39 J/°CA, respectively, at an injection time of 25 °bTDC.
- The B20+ CuO75+QPAN75 has portrayed the inferior CO, UHC, NO_x, and smoke of about 0.089 %, 32 ppm, 1238 ppm, and 19.351 %, respectively, at an injection time of 25 °bTDC.

According to the results, a compression ignition engine can be operated without modifications with the dispersion of CuO nanoparticles in *Azadirachta indica* biodiesel blend (B20) combined with the dispersants.

Funding

Not applicable.

Code availability

Not applicable.

CRediT authorship contribution statement

Ramu Garugubilli: Conceptualization, Formal analysis, Investigation, Methodology, Writing – original draft. **Vanthala Varaha Siva Prasad:** Conceptualization, Data curation, Formal analysis, Investigation, Methodology, Resources, Supervision, Validation, Writing – original draft, Writing – review & editing. **Jaikumar Sagari:** Conceptualization, Data curation, Methodology, Resources, Supervision, Validation, Writing – original draft, Writing – review & editing.

Declaration of competing interest

The authors have no conflict interest.

Data availability

No data was used for the research described in the article.

References

[1] Ü. Ağbulut, S. Sarıdemir, U. Rajak, F. Polat, A. Afzal, T.N. Verma, Effects of high-dosage copper oxide nanoparticles addition in diesel fuel on engine characteristics, Energy 229 (2021) 120611.
[2] A. Al Ezzi, M.A. Fayad, A.M. Al Jubori, A.A. Jaber, L.A. Alsadawi, H.A. Dhahad, T Yusaf, Influence of fuel injection pressure and RME on combustion, NOx emissions and soot nanoparticles characteristics in common-rail HSDI diesel engine, Int. J. Thermofluids 15 (2022) 100173.
[3] S. Jaikumar, V. Srinivas, R.S. Meher, Combustion characteristics of direct injection diesel engine fueled with dispersant-mixed Al_2O_3 nanoparticle-added biodiesel blend, Int. J. Thermophys 42 (6) (2021) 1–15.
[4] M.A. Mujtaba, M.A. Kalama, H.H. Masjuki, M. Gul, M.E.M. Soudagar, C.O. Hwai, A. Waqar, A.E. Atabani, L. Razzaq, Y. Mnam, Comparative study of nanoparticles and alcoholic fuel additives-biodieseldiesel blend for performance and emission improvements, Fuel 279 (2020) 118434.
[5] R. Madihi, M. Pourfallah, M. Gholinia, M. Armin, A.Z. Ghadi, Thermofluids analysis of combustion, emissions, and energy in a biodiesel (C11H22O2)/natural gas heavy-duty engine with RCCI mode (Part II: fuel injection time/Fuel injection rate), Int. J. Thermofluids 16 (2022) 100200.
[6] S.A. Basha, K.R. Gopal, S. Jebaraj, A review on biodiesel production, combustion, emissions and performance, Renew. Sustain. Energy reviews 13 (6–7) (2009) 1628–1634.
[7] A.S. Vinayaka, B. Mahanty, E.R. Rene, S.K. Behera, Biodiesel production by transesterification of a mixture of pongamia and neem oils, Biofuels (2018).
[8] U. Agbulut, M. Karagoz, S. Sarıdemir, A. Oztürk, Impact of various metal- oxide based nanoparticles and biodiesel blends on the combustion, performance, emission, vibration and noise characteristics of a CI engine, Fuel 270 (2020) 117521.

[9] S.H. Shariff, S. Vadapalli, J. Sagari, Experimental study on direct injection diesel engine fuelled with ferric chloride nanoparticle dispersed *Cassia Fistula* biodiesel blend, Int. J. Energy Environ. Eng. (2021), https://doi.org/10.1007/s40095-021-00405-0.
[10] K. Sanatha, S.K. Bhatti, S. Jaikumar, Influence of ZnO nanoparticles and dispersant in Baheda oil biodiesel blend on the assessment of performance, combustion, and emissions of VCR diesel engine, Appl. Nanosci. (2021), https://doi.org/10.1007/s13204-021-02233-4.
[11] A.M. Ansari, L.A. Memon, M.T. Ghannam, M.Y. Selim, Impact of biodiesel blended fuel with nanoparticles on performance and noise emission in compression ignition engine, Int. J. Thermofluids (2023) 100390.
[12] V.K. Nema, A. Singh, Emission reduction in a dual blend biodiesel fuelled CI engine using nano-fuel additives, Mater. Today: Proc. 5 (9) (2018) 20754–20759.
[13] K. Jagadish, Varaha Siva Prasad Vanthala, Jaikumar Sagari, The effect of a surfactant and dispersant mixed Cr2O3 nanoparticles on the analysis of stability and physicochemical properties of a Mesuaferrea biodiesel blend, Pet. Sci. Technol. (2022), https://doi.org/10.1080/10916466.2022.2117381.
[14] I. Madhavi, S.V.P. Lankapalli, J. Sagari, Influence of dispersant-mixed TiO_2 nanoparticles on stability and physicochemical properties of Semecarpus anacardium biodiesel blend, Int. Nano Lett. (2022), https://doi.org/10.1007/s40089-022-00384-y.
[15] V. Praveena, M.L.J. Martin, V.E. Geo, Experimental characterization of CI engine performance, combustion and emission parameters using various metal oxide nanoemulsion of grapeseed oil methyl ester, J. Therm. Anal. Calorim. 139 (6) (2020) 3441–3456.
[16] S. Jaikumar, V. Srinivas, M. Rajasekhar, Influence of dispersant added nanoparticle additives with diesel-biodiesel blend on direct injection compression ignition engine: combustion, engine performance, and exhaust emissions approach, Energy 224 (2021) 120197.
[17] K. Nanthagopal, B. Ashok, Ajith J.A Tamilarasu, M. Aravind, Influence on the effect of zinc oxide and titanium dioxide nanoparticles as an additive with Calophylluminophyllum methyl ester in a CI engine, Energy Convers. Manage 146 (2017) 8–19.
[18] V. Perumal, M. Ilangkumaran, The influence of copper oxide nano particle added pongamia methyl ester biodiesel on the performance, combustion and emission of a diesel engine, Fuel 232 (2018) 791–802.
[19] A. Praveen, G.L.N. Rao, B. Balakrishna, Performance and emission characteristics of a diesel engine using Calophyllum inophyllum biodiesel blends with TiO2 nanoadditives and EGR, Egypt. J. Petrol. 27 (4) (2018) 731–738.
[20] M. Illipilla, S.V.P. Lankapalli, J. Sagari, Experimental study on a diesel engine fueled with Semecarpus anacardium biodiesel containing dispersed TiO2 nanoparticles: performance, combustion, and emission analyses, Energy Ecol. Environ. 8 (2) (2023) 113–128.
[21] S. Jaikumar, S.K. Bhatti, V. Srinivas, R. Satyameher, S.B. Padal, D. Chandravathi, Combustion, vibration, and noise characteristics of direct injection VCR diesel engine fuelled with Mesua ferrea oil methyl ester blends, Int. J. Ambient Energy 43 (2020) 1–12.
[22] S.R. Pala, V.S.P. Vanthala, J. Sagari, Influence of dispersant and surfactant added graphene oxide nanoparticles on Mahua biodiesel blend: stability and physicochemical properties approach, Emergent. Mater. (2023) 1–9.
[23] V.L. Reddy, J. Sagari, S. Vadapalli, V.V.S. Prasad, Application of response surface methodology to the operating parameters of diesel engines fueled with SiO2 nanoparticles in Abrus precatorius biodiesel, Emergent. Mater. (2023) 1–16.
[24] S. Jaikumar, V. Srinivas, V.V.S. Prasad, G. Susmitha, P. Sravya, A. Sajala, L. Jaswitha, Experimental studies on the performance and emission parameters of a direct injection diesel engine fuelled with nanoparticle-dispersed biodiesel blend, Nanotechnol. Environ. Eng. 6 (1) (2021) 1–17.
[25] J. Kari, V.S.P. Vanthala, J. Sagari, The influence of Cr_2O_3 nanoparticles dispersed Mesua ferrea biodiesel on the analysis performance, combustion, and emissions of diesel engine, Environ. Dev. Sustain. (2023) 1–27.
[26] S.H. Hosseini, A. Taghizadeh-Alisaraei, B. Ghobadian, A. Abbaszadeh-Mayvan, Performance and emission characteristics of a CI engine fuelled with carbon nanotubes and diesel-biodiesel blends, Renew. Energy 111 (2017) 201–213.
[27] M. Nour, A.I. El-Seesy, A.K. Abdel-Rahman, M. Bady, Infuence of adding aluminum oxide nanoparticles to diesterol blends on the combustion and exhaust emission characteristics of a diesel engine, Exp. Therm. Fluid. Sci. 98 (2018) 634–644.
[28] A.F. Chen, M.A. Adzmi, A. Adam, M.F. Othman, M.K. Kamaruzzaman, A.G. Mrwan, Combustion characteristics, engine performances and emissions of a diesel engine using nanoparticlediesel fuel blends with aluminium oxide, carbon nanotubes and silicon oxide, Energy Convers. Manage 171 (2018) 461–477.
[29] K. Tina, K.K. Anita, K. Breda, K. Marko, Nanomaterials as fuel additives in diesel engines: a review of current state, opportunities, and challenges, Prog. Energy Combust. Sci. 83 (2021) 100897.
[30] S. Kumar, P. Dinesha, I. Bran, Infuence of nanoparticles on the performance and emission characteristics of a biodiesel fuelled engine: an experimental analysis, Energy 140 (2017) 98–105.
[31] B. Prabakaran, P. Vijayabalan, Infuence of zinc oxide nano particles on performance, combustion and emission characteristics of butanol-diesel-ethanol blends in DI CI engine, in: IOP Conference Series: Materials Science and Engineering 377, IOP Publishing, 2018 012069.
[32] A.I. EL-Seesy, H. Hassan, S.J.E.C. Ookawara, Performance, combustion, and emission characteristics of a diesel engine fueled with Jatropha methyl ester and graphene oxide additives, Energy Convers. Manage. 166 (2018) 674–686.
[33] S. Jaikumar, S.K. Bhatti, V. Srinivas, R. Satyameher, D. Chandravathi, Investigations on performance and emission parameters of direct injection diesel engine running with Mesua ferrea oil methyl ester blends, SN. Appl. Sci. 1 (11) (2019) 1–7.
[34] M.E.M. Soudagar, N.N. Nik-Ghazali, M.A. Kalam, I.A. Badruddin, N. R. Banapurmath, N. Akram, The efect of nano-additives in diesel-biodiesel fuel blends: a comprehensive review on stability, engine performance and emission characteristics, Energy Convers. Manage 178 (2018) 146–177.